



# Experimental comparison of fiber optic parametric, Raman and erbium amplifiers for burst traffic for extended reach PONs

CHANDRA B. GAUR,<sup>1,\*</sup> FILIPE FERREIRA,<sup>1,2</sup>  VLADIMIR GORDIENKO,<sup>1</sup>  VITOR RIBEIRO,<sup>1</sup> ÁRON D. SZABÓ,<sup>1</sup> AND NICK J. DORAN<sup>1</sup>

<sup>1</sup>Aston Institute of Photonics Technology, Aston University, Birmingham B4 7ET, UK

<sup>2</sup>Now with University College London (UCL), Gower Street, London WC1E 6BT, UK

\*gaurc@aston.ac.uk.

**Abstract:** We experimentally compare the performance of a polarization-independent fiber optic parametric amplifier (FOPA), a discrete Raman amplifier and a commercial erbium doped fiber amplifier (EDFA) for burst traffic amplification in extended reach passive optical networks (PON). We demonstrate that EDFA and Raman amplifiers suffer from severe transient effects, causing penalty on receiver sensitivity  $>5$  dB for traffic bursts of 10 Gbps on-off keying signal shorter than 10  $\mu$ s. On the other hand, we demonstrate that FOPA does not introduce a penalty on receiver sensitivity when amplifying signal bursts as short as 5  $\mu$ s as compared to a non-burst signal. Therefore, FOPA used as a drop-in replacement for an EDFA or Raman amplifier allows us to improve receiver sensitivity by  $>3$  dB for short signal bursts. We conclude that FOPA allows substantially increased power budget for an extended reach PON transmitting variable duration bursts. In addition, we identify the maximum burst duration tolerated by each examined amplifier.

Published by The Optical Society under the terms of the [Creative Commons Attribution 4.0 License](https://creativecommons.org/licenses/by/4.0/). Further distribution of this work must maintain attribution to the author(s) and the published article's title, journal citation, and DOI.

## 1. Introduction

Fiber optic parametric amplifiers (FOPA) have been shown to be a promising amplification technology for fiber optical communication with such unique features as a very large gain (70 dB) [1,2] a broad ( $>100$  nm) and flat gain spectrum [3–5], and phase sensitive gain allowing for  $<3$  dB noise figure [6]. FOPA has recently become available for in-line amplification with introduction of novel polarization-insensitive FOPA architectures [7–9]. FOPA reliance on Kerr effect allows for practically instantaneous response time of  $\sim 0.1$  fs thus avoiding penalties on amplification of traffic bursts [10]. In addition, the FOPA ability to operate in arbitrary wavelengths bands [11] makes it appealing for passive optical networks (PONs) utilizing O, C and L bands [4,11]. This opens a promising application of parametric amplification as in-line amplifier for reach extended passive optical network (PON).

PON has provided a cost efficient medium for high speed optical data transmission. Extended reach PON is envisaged to consolidate a large number of central office locations into a few access nodes to reduce operational expenditure [12]. Reach extension could converge multiple number of users into a single access layer node, therefore a split ratio increase is required too [12]. An in-line optical amplification was proposed to extend a reach of symmetrical XGS-PON (10G-PON) and above up to 60 km [13] and to enable a required split ratio increase [14]. Although the reach is limited by a chromatic dispersion too [15,16] the impact of chromatic dispersion can be mitigated by using advance digital signal processing (DSP) techniques and high sensitivity coherent receivers [17].

There are a few specific requirements for amplifiers employed in an extended reach PONs. The key requirement is an ability to amplify an upstream consisting of data bursts [18]. Another requirement is to provide high output powers to allow for a high splitting ratio. An ability to operate in O, E, S, C and L bands might be required too as PON technologies employ these transmission bands [19]. Semiconductor optical amplifiers (SOA), EDFA and Raman amplifiers are considered for employment in extended reach PON to increase its power budget [20–22]. SOAs can operate in all bands appealing for PON, and SOAs are compatible with burst amplification due to fast response time, but their nonlinear behavior at high signal powers limits splitting ratios in PON [23]. EDFAs allow for good performance and high output powers [24] but their slow response time about a few hundreds of microseconds [25] imposes limitations on amplification of signal bursts [26]. Distributed and discrete Raman amplifiers have been proposed for extended reach PON [23,27] but they can suffer from transient effects when amplifying signal bursts too. Response time of Raman amplifiers may greatly exceed that of Raman scattering due to a relative motion between a pump and a signal waves over a long 6.5 km gain section [27,28]. We propose to employ FOPA as an amplifier for extended reach PON, because it can satisfy all the requirements: to amplify signal bursts without degrading them by transient effects to provide a high output power [29,30] and to operate across multiple wavelength bands [31,32]. Transient effects in EDFA and Raman amplifier have again been analyzed in this experiment to provide a reference point and to show improvement provided by FOPA.

In this paper we extend our previous work [33,34] experimentally demonstrating a polarization-insensitive FOPA (PI-FOPA) as a drop-in replacement amplifier for amplification of a bursty traffic in extended reach PON. We transmit a bursty 10 Gbps on-off keying (OOK) signal by 50 km, amplify it by FOPA, a discrete Raman amplifier or a commercial EDFA, before passing it through a variable optical attenuator (VOA) emulating a PON splitter, and detect the signal. At the receiver we count errors and derive its sensitivity for each amplifier to assess its performance. We investigate non-burst and range of bursts duration from 5 to 70  $\mu\text{s}$  and demonstrate that while EDFA and Raman amplifier can suffer from significant penalties due to transient effects. PI-FOPA has little penalties when amplifying bursty traffic thanks to its practically instantaneous response time. Overall, we demonstrate PI-FOPA to improve receiver sensitivity by at least 3 dB as compared with discrete Raman amplifier and EDFA thus allowing for longer reach and/or higher splitter ratios.

## 2. Experimental setup

Figure 1 shows an experimental setup to compare performance of EDFA, Raman amplifier and FOPA for extended reach PON. The experimental setup consisted of a bursty traffic transmitter, a 50 km transmission line and an amplifier under test (AUT) followed by a VOA emulating a splitter and a receiver.

The transmitter produced bursts of a 10 Gbps OOK signal. The signal in the transmitter was sourced from a 100 kHz linewidth laser at wavelength of 1535 nm and modulated by a Mach-Zehnder modulator (MZM) at 10 Gbps using OOK. The MZM was driven with a pseudo random bit sequence (PRBS)  $2^{11}-1$  bits long. Then, the signal was amplified by a booster EDFA with output power of 13 dBm. Traffic bursts were emulated by passing the signal through an acousto-optic modulator (AOM) driven by an external waveform generator producing a variable duty cycle square wave at frequency of 10 kHz. The AOM insertion loss was 5.5 dB and the rise time was 10 ns. The rise time was fast enough to create bursts with a leading edge sufficiently sharp to investigate transients of the tested amplifiers. The period of bursts was 100  $\mu\text{s}$  and the duration of bursts could be varied from 5  $\mu\text{s}$  to 70  $\mu\text{s}$  (Fig. 2). A typical burst duration in PONs with a 10G upstream is between 0.5  $\mu\text{s}$  and 125  $\mu\text{s}$  [35]. We have examined most of this range by sweeping burst duration from 5  $\mu\text{s}$  to 70  $\mu\text{s}$  as is allowed by the equipment and have observed FOPA to introduce little penalties. We expect FOPA to deliver similar performance for bursts

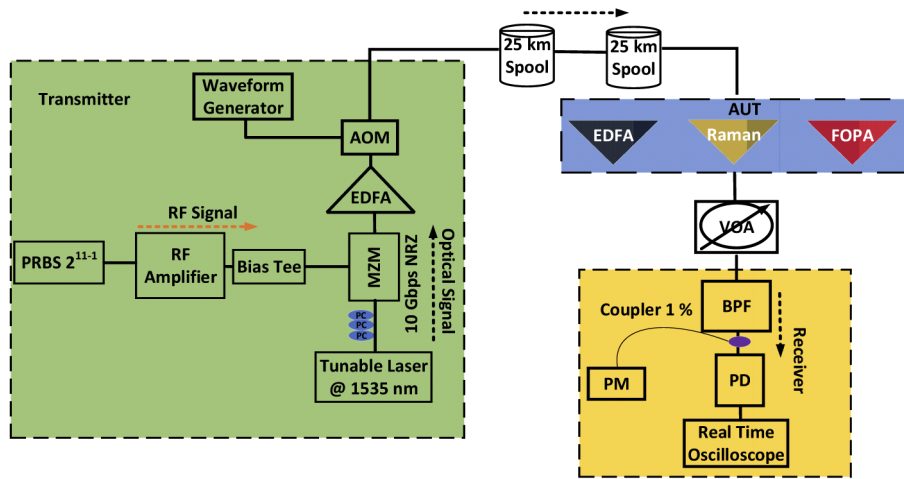


**Fig. 1.** Experimental setup to compare performance of EDFA, Raman amplifier and FOPA in extended reach PON scenario featuring burst traffic transmitter and transmission over 50 km.

duration down to 0.5  $\mu\text{s}$  since the FOPA response time is of the order of femtoseconds. The average power after the AOM was a product of the burst power fixed at 7.5 dBm and the duty cycle, e.g. the average power was -2.5 dBm for 10% duty cycle. Figure 2 shows a schematic representation of emulated signal burst with burst duration of 10, 30 or 50  $\mu\text{s}$  and a burst period of 100  $\mu\text{s}$ . Non-burst traffic was produced in the same setup by setting the waveform generator duty cycle to 100%.

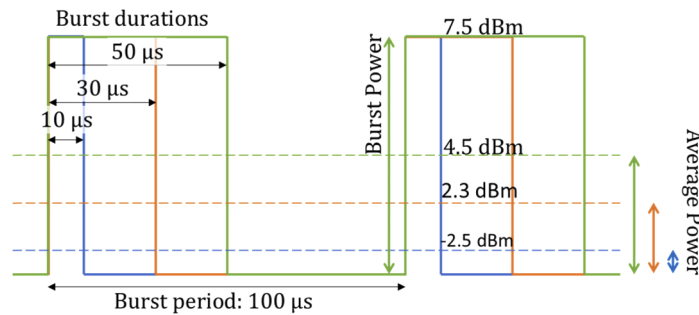


**Fig. 2.** Schematic representation of emulated signal bursts with burst durations of 10, 30 or 50  $\mu\text{s}$  and a burst period of 100  $\mu\text{s}$ .

The generated burst traffic was transmitted over 50 km of a standard single mode fiber with a total loss of 9.7 dB and amplified by one of AUTs. Signal burst power at the AUT input was therefore fixed at -2.2 dBm. Two sets of results were obtained: (i) all AUTs set to 13 dB net gain and (ii) all AUT set to 20 dB gain except the Raman amplifier unable to deliver 20 dB net gain. The amplified burst power was therefore either 10.8 dBm or 17.8 dBm. Then, amplified signals were attenuated by a VOA emulating an optical splitter. Attenuation of the VOA was varied to sweep the power at a receiver. In the back-to-back (B2B) scenario the transmission fiber and AUTs were bypassed, so the transmitter was connected directly to the VOA preceding the receiver.

The polarization insensitive FOPA (Fig. 3(a)) employed a polarization diversity loop architecture [9]. An input signal was split by a polarization beam splitter (PBS) into orthogonal polarization components. Each polarization component was independently and equally amplified in one of two highly nonlinear fibers (HNLF). The HNLFs had zero-dispersion wavelength of  $\sim 1564$  nm and nonlinearity of  $8.2 \text{ W}^{-1}\text{km}^{-1}$ . After propagating through a complete loop, the amplified polarization components were recombined by the PBS. The HNLFs insertion loss were 1.4 dB and 0.9 dB, and lengths were 250 m and 200 m respectively. A seed for pumps was sourced from a 100 kHz linewidth laser and phase modulated with three tones at 100, 320 and 980 MHz to mitigate stimulated Brillouin scattering (SBS) [8]. Then, the seed was split by a 3 dB coupler into two waves amplified by two high-power EDFAs to produce two pumps. HNLFs were 34.5 dBm and 33.1 dBm respectively to achieve 13 dB net gain or 34.8 dBm and 33.8 dBm to achieve 20 dB net gain.

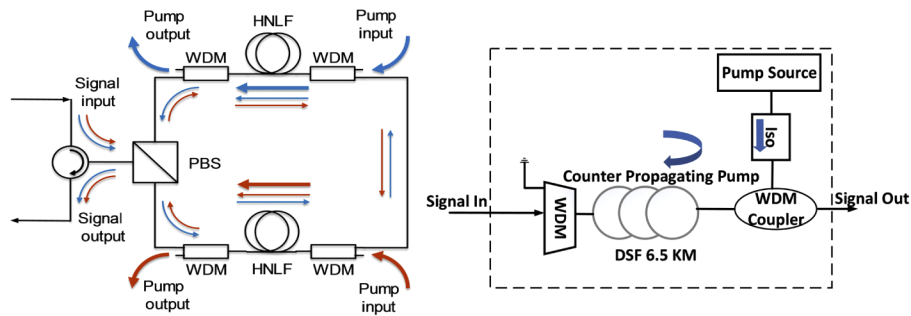


**Fig. 3.** Experimental setup of (a) polarization independent FOPA [9] and (b) discrete Raman amplifier [31].

The EDFA was a commercial in-line two stage EDFA with maximum output power of 23.5 dBm and 23 dB gain. The EDFA has a noise figure of 5.5 dB, a built-in dynamic gain control and a guaranteed transient settling time under 1 ms. In this experiment we employ an EDFAs with automatic gain control allowing for a transient settle time down to  $\sim 1 \mu\text{s}$  [26]. Moreover, EDFAs with sub- $\mu\text{s}$  response time are available to suppress gain fluctuations due to channel add/drop operations. However, such EDFAs are limited to a narrow operation bandwidth of a few nm, and typically are not intended for significant power fluctuations  $>6$  dB occurring at the burst edges. Nevertheless, the FOPA given its fast response time will be able to amplify very short bursts lengths without transient. The Raman amplifier was backward pumped by a 2.8 W pump at 1452 nm (Fig. 3(b)). The Raman gain fiber was a 6.5 km long dispersion shifted fiber (DSF) with a zero-dispersion wavelength at 1542 nm. 1450/1550 nm WDM couplers were employed at the ends of the Raman gain fiber to couple in and to couple out the pump respectively. The Raman amplifier net gain was 13 dB. It was not possible to achieve net gain of 20 dB in this Raman amplifier setup without incurring lasing.

The receiver (Fig. 1) employed a band pass filter (BPF) with a bandwidth of 1 nm tuned to the signal wavelength. The signal power was monitored after the BPF by a power meter connected via a calibrated 1% tap coupler. Then, the signal was detected by a PIN photodetector with responsivity of 0.3 A/W and captured using a real time sampling oscilloscope with bandwidth of 23 GHz. The received signal was then processed offline to detect bursts, set a decision threshold and to count errors. The bit error rate (BER) was measured versus a range of received signal powers for each AUT. Eventually, receiver sensitivity is derived as a received signal burst power when BER is  $10^{-3}$ . Better receiver sensitivity means that higher attenuation of VOA (or splitter) is supported.

### 3. Experimental results and discussion

In this section performance of AUTs for amplification of signal bursts with varied duration is analyzed. Results obtained for the B2B configuration and with non-burst signals are used for a reference. First, waveforms of signal bursts are analyzed for each of six scenarios investigated in the paper (i) B2B (ii) EDFA with 20 dB and 13 dB gain (iii) Raman with 13 dB gain (iv) FOPA with 20 dB and 13 dB gain. Second, performance of each AUT is analyzed via BER measurements. BER was calculated via error counting across ten signal bursts captured by a real time oscilloscope. Finally, the receiver sensitivity defined as the signal power required for BER of  $10^{-3}$  is found as a function of a signal burst duration for each AUT.

#### 3.1. Characterization of burst waveform

Figure 4 shows waveforms of the signal bursts at the receiver in the six scenarios investigated in this paper as mentioned above. The waveforms were captured with a real time oscilloscope with sampling rate of 100 GS/s. Bursts in B2B configuration have a clear rectangular shape. However, waveforms of bursts amplified by EDFA and Raman are distorted by substantial gain variation along the bursts. These distortions are presumably caused by the EDFA and the Raman amplifier response time [26,27]. Raman amplifier with counter propagation of pump and signal demonstrate longer response time due to propagation delay in Raman gain medium. In the EDFA and the Raman cases the top of the bursts is clearly sloped from the leading edge of the burst till the end of the burst. Therefore, the transient is not settled within the burst duration of 30  $\mu$ s. On the other hand, in the case of amplification by FOPA the bursts are not distorted. A pattern of the FOPA amplified bursts seen in Fig. 4(e) and (f) follows those observed in B2B Fig. 4(a). Therefore, we conclude this pattern stems from the transmitter or the receiver. The absence of burst distortions in the FOPA case demonstrates the ability of the FOPA to deliver practically instantaneous dynamic gain required for transmission of bursty traffic in PON.

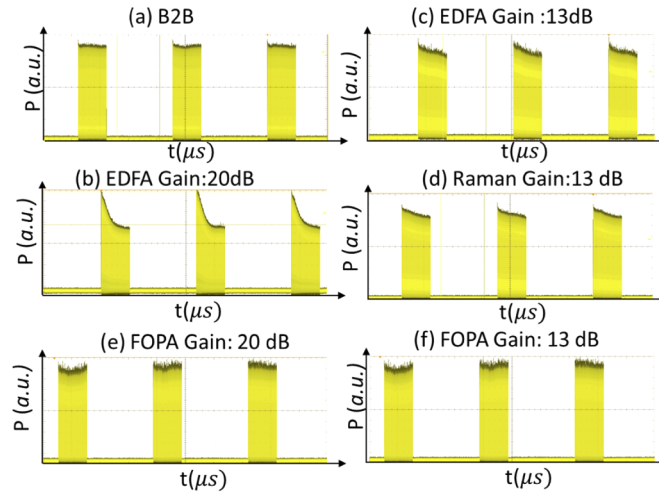


**Fig. 4.** Waveforms of signal bursts captured by a real time oscilloscope at the receiver in six scenarios: B2B (a); transmission and 20 and 13 dB amplification by EDFA (b) and (c), and Raman 13 dB gain (d); transmission and 20 and 13 dB gain (e) and (f).

#### 3.2. Characterization of burst BER

Performance of each AUT was analyzed via BER measurements with a non-burst signal and with burst signal durations of 10  $\mu$ s, 30  $\mu$ s and 50  $\mu$ s to evaluate an impact of transients on bursty



signal for each AUT. The non-burst signal was investigated along with bursty signals to provide a baseline for studying transient effects in standalone AUT. The BER was calculated over a period of 1 ms. Consequently, the number of analyzed bits varied from  $10^7$  for non-burst signals to  $10^6$  for 10  $\mu\text{s}$  signal bursts. Figure 5 shows fluctuations of leading bits in B2B burst for 100 ns introduced by the AOM, the bits in this fluctuating time are discarded before error counting for all cases. The threshold detection was performed as described in [36] with an auto threshold control function capable of 50 ns settling time.

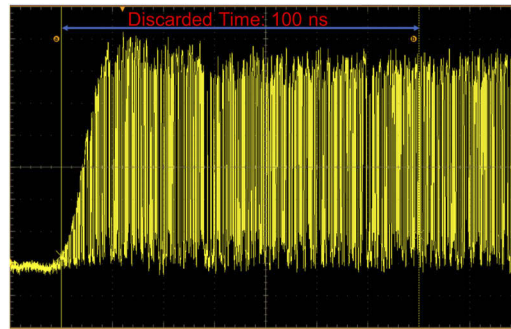


**Fig. 5.** Oscilloscope view of the 30  $\mu\text{s}$  burst in the B2B arrangement shows distortion of the burst due to transients in the AOM and the receiver. The first 100 ns of the burst are therefore discarded from the analysis for all scenarios.

Figure 6 shows measured BER versus an average burst power in the B2B configuration and with each of tested amplifiers set to 13 dB gain. In the B2B scenario the 50  $\mu\text{s}$  signal bursts required  $\sim 2$  dB higher average signal power at the receiver than the non-burst signal to achieve the same BER (Fig. 6(a)). As the burst's duration decreased the power penalty increased and reached  $\sim 3$  dB for the 10  $\mu\text{s}$  burst. This performance degradation in the burst implementation penalty which needs to be accounted for when comparing performance of AUTs in non-burst and burst scenarios. The most likely source of this penalty was the PIN receiver not optimized for burst traffic [37]. This non-optimization of the receiver creates longer reception of fast incoming bits arriving at leading edges of the bursts [36].

In the scenario with 13 dB amplification by EDFA a bursty signal suffered from significant degradation as compared to a non-bursty signal (Fig. 6(b)). The 50  $\mu\text{s}$  signal bursts required  $\sim 3$  dB higher signal power at the receiver than the non-burst signal to reach BER of  $10^{-3}$ . This penalty increased to 8 dB as the burst duration was decreased to 10  $\mu\text{s}$ . In addition, the power penalties on bursty signals were much higher at lower BER levels placing BER of just  $10^{-4}$  out of reach in case of the 10  $\mu\text{s}$  long signal bursts. Overall, an addition of EDFA to the setup has significantly degraded BER of the bursty signals in comparison with the moderate 2-3 dB burst implementation penalty demonstrated in the B2B case. Also, to note low net gain of 13 dB introduce high noise figure in EDFA ( $>7.7$  dB) which contributed to BER penalty observed in the values shown in the figure.

In the case of the discrete Raman amplifier the maximum received power penalty suffered by the 50  $\mu\text{s}$  and the 30  $\mu\text{s}$  bursts were about 1-2 dB (Fig. 6(c)) and therefore BER follows very similar power dependency as the B2B scenario. Consequently, the degradation of BER for the 50  $\mu\text{s}$  and the 30  $\mu\text{s}$  bursts was mainly due to limitations of the receiver rather than due to amplification by the Raman amplifier, since stimulated Raman scattering (SRS) effect have instantaneous response time with femtosecond time scale ( $<100$  fs) where propagational delay not effective with respect to burst duration [38]. For large gain and transmission capacity backward pumped discrete Raman fibre amplifiers are preferred specifically in metro and access applications [23]. However, Fig. 6(c) demonstrates that 10  $\mu\text{s}$  signal bursts suffered from significant BER degradation as

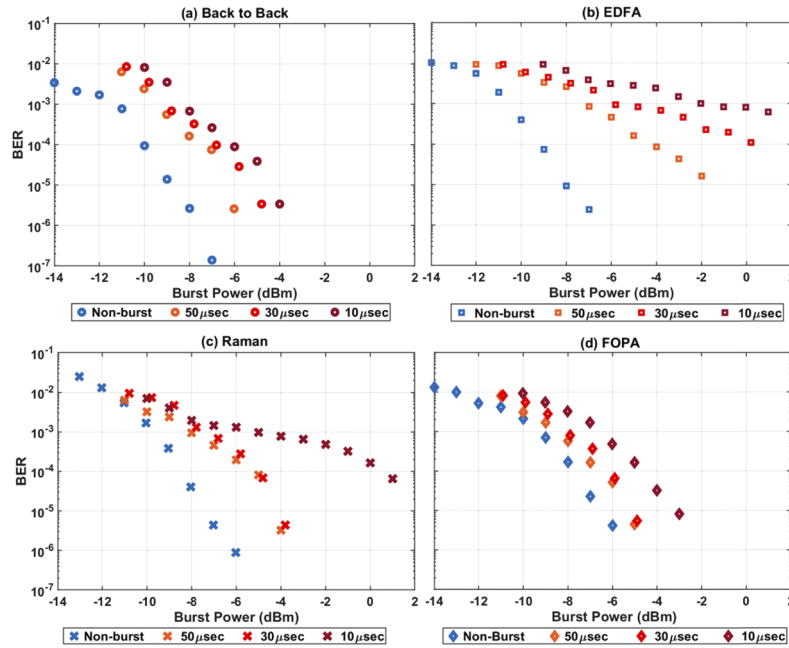


**Fig. 6.** Experimental comparison of BER vs average burst power show an impact of (b) EDFA (d) FOPA and (c) Raman amplifier on signal bursts. Results in the B2B scenario (a) are provided for a reference. Burst durations of 50  $\mu$ s, 30  $\mu$ s and 10  $\mu$ s are investigated and compared to performance of non-burst (continuous) signal. Gain of tested amplifiers was 13 dB.

the signal power increased. This is attributed to transient arising in backward pumped Raman amplifiers due to time required for the pump and the signal to propagate along a gain fiber [39]. In the tested Raman amplifier, the propagation time through the 6.5 km long gain fiber is 32  $\mu$ s at the signal wavelength. Therefore, although the discrete Raman amplifier response time is faster than that of the EDFA, it is still on the scale of the traffic bursts duration. Overall, the tested discrete Raman amplifier is more robust to transients than the EDFA, but it is still susceptible to transients in short bursts with durations comparable with the propagation time in the Raman amplifier. Robustness of the discrete Raman amplifier against transients can be improved by using either a forward pumping scheme or a shorter gain fibre [40].

In case of the FOPA the difference between the received signal powers required to achieve the same BER for non-burst and for burst signals is under 3 dB in all cases quite similarly to the B2B scenario (Fig. 6(d)). Therefore, the BER difference between burst and non-burst signals is mainly attributed to performance limitations of the non-burst mode receiver. On the contrary, for the overall investigated power range tested for FOPA has not introduced an additional power penalty of bursty signals from typical value of 0 dB to maximum value of 1 dB thus confirming the lack of transient effects in FOPA. Overall, the instantaneous response of the FOPA makes it very appealing for amplification of burst signals.

Figure 7(a) shows BER comparison for non-burst signals amplified by 13 dB gain plotted together with the B2B case in non-burst mode. Input signal power to each AUT was -2.2 dBm with output amplified power of 10.8 dBm. Non-burst performance analysis provided base line for standalone amplifier performance in transmission setup. Improved performance of EDFA was noticed for non-burst mode in comparison with Raman and FOPA. 1 dB performance penalty was noticed between B2B and EDFA amplified signal and <1 dB penalty observed between all AUTs for the overall investigated power range. Almost similar power penalty was observed for Raman

and FOPA in non-burst mode. Minor penalty in non-burst mode performance from B2B indicates isolation of other effects in AUTs like noise figures, dispersion penalty and nonlinearity stem from transmission fiber. A maximum delay between the signal frequency components due to dispersion was about 85 ps being calculated as a product of the SSMF dispersion of 17 ps/nm/km, a measured signal bandwidth of 0.1 nm and the transmission fiber length of 50 km. A bit duration of a 10 Gbps signal is 100 ps, so the delay introduced by dispersion of the transmission fiber is still less than the bit duration but might introduce a performance penalty [15]. A nonlinear phase shift of the signal was  $\sim 0.2$  rad being calculated as a product of: the SSMF nonlinearity coefficient of  $0.78 \text{ W}^{-1} \cdot \text{km}^{-1}$  [41], the transmission fiber effective length of 23 km, and the peak input signal power of 10.5 dBm (11.2 mW). Value of non-linearity in 50 km SMF was tolerable to transmit signal without any observable signal broadening for effective length of 23 km.

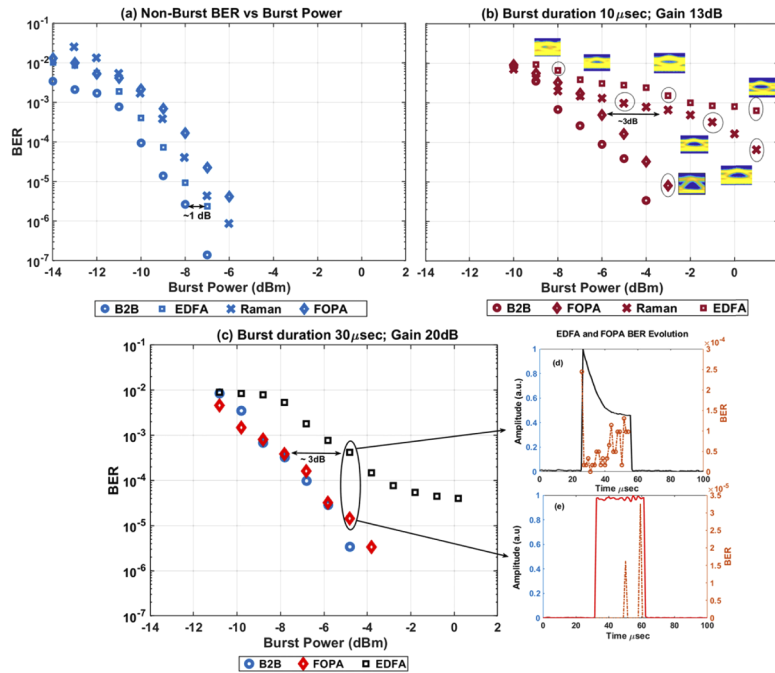


**Fig. 7.** BER vs average burst power for B2B and each AUT for (a) Non-burst mode with 13 dB gain (b) burst duration of 10  $\mu\text{s}$  and AUTs gain of 13 dB with inset eye diagrams (c) burst duration of 30  $\mu\text{s}$  and AUTs gain of 20 dB (except Raman). EDFA and FOPA BER evolution shown in 30  $\mu\text{s}$  bursts in (d) and (e). BER averaged across ten signal bursts

Figure 7(b) shows a BER comparison for 10  $\mu\text{s}$  signal bursts in the B2B scenario and after amplification with each AUT by 13 dB. FOPA has performed with less than 1 dB penalty on the received signal power as compared to the B2B configuration across all studied BER range. On the contrary, bursts amplified by the discrete Raman amplifier and the EDFA have suffered from significant degradation. Thus, for BER better than  $10^{-3}$ , over 3 dB and 5 dB higher signal power at the receiver was required in the Raman and the EDFA cases respectively to achieve the same BER as in the FOPA case. Eye diagrams shown on the inset demonstrate that for signal power of -3 dBm the FOPA case provides a clear open eye corresponding to a BER of  $10^{-5}$ , while the EDFA and the Raman cases have almost closed eye diagrams corresponding to a BER of  $10^{-3}$ .

Figure 7(c) shows a BER comparison for 30  $\mu\text{s}$  signal bursts in the B2B scenario and after amplification by the EDFA and the FOPA by 20 dB. The discrete Raman amplifier is not compared here as it was not able to deliver 20 dB net gain. The FOPA does not show any observable



penalty as compared to the B2B scenario. B2B and FOPA curves are within measurement error from each other. On the contrary, the EDFA suffers from the 3 dB power penalty at the BER level of  $10^{-3}$  and shows signs of a performance floor at BER of  $10^{-4}$  due to occurrence of transient. Figures 7(d) and (e) show BER across sample bursts amplified by the EDFA or the FOPA at received signal power of -5 dBm. It is evident that in the FOPA case there are only a few occasional errors with overall BER of  $\sim 10^{-5}$ , while in the EDFA case errors occur continuously throughout the bursts resulting in overall BER of  $\sim 10^{-4}$ . Figure 6(b) and Fig. 7(c) are compared for 30  $\mu$ s burst amplification with 13 dB and 20 dB gain. EDFA with 13 dB gain at received signal power above -3 dBm shows higher penalty in BER values in comparison with 20 dB gain. This is due to the inclusion of high noise figure in EDFA at low gain amplification of burst signal. Whereas, FOPA at both gain levels (13 and 20 dB) shows consistent performance in BER values. Overall, the FOPA shows a superior performance even for net gain of 20 dB.

### 3.3. Signal burst duration and receiver sensitivity

Figure 8 shows the receiver sensitivity from B2B to each AUT at 13 dB gain as a function of signal burst duration. The receiver sensitivity is defined as the required average signal power to reach BER of  $10^{-3}$  from B2B. The sensitivity is one of the most important parameters in PON defining the available power budget and consequently the reach and the maximum available splitting ratio. A range of burst durations from 70  $\mu$ s to 5  $\mu$ s as well as a non-burst signal were analyzed. The B2B receiver sensitivity provides a baseline for performance of all AUTs. Thus, the receiver sensitivity for a non-burst signal is -12 dBm, but for bursty signals it is up to 2 dB worse reaching -10 dBm for durations under 50  $\mu$ s reasonably due to the limitation in photodetector switching in burst mode. EDFA and Raman amplifier due to the occurrence of transient effects shows  $\sim 3$  dB sensitivity penalty from B2B at -6 dBm. Large penalties (5-8 dB) on short burst makes them non-recoverable due to large BER degradation. Which makes the system non-performable to recover short bursts without scarifying 5-8 dB of the power budget.

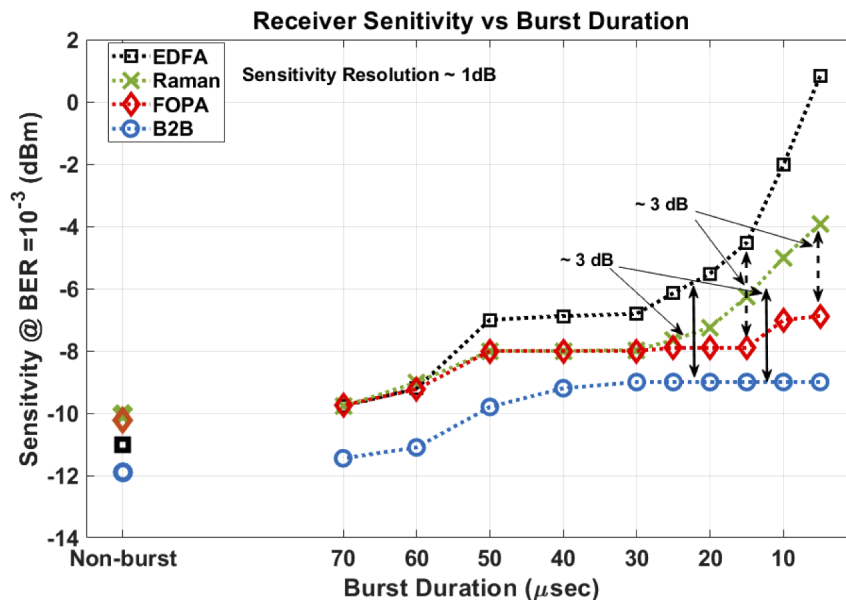


**Fig. 8.** Plot shows receiver sensitivity vs burst durations from 5  $\mu$ s to 100  $\mu$ s (non-burst) at BER level of  $10^{-3}$  marked 3 dB degradation in EDFA and Raman receiver sensitivity at different burst durations.

FOPA on the other hand has a stability factor of 1 dB sensitivity change from B2B for burst duration lengths from 70  $\mu$ s to 15  $\mu$ s.

As previously seen, due to the fast response time of FOPA negligible dependency on various burst durations was achieved, although for burst durations below 10  $\mu$ s additional noise occurred due to FOPA polarization diversity loop architecture. EDFA adds power penalty of 3 dB for burst durations below 20  $\mu$ s from FOPA and this increases severely by 7 dB for 5  $\mu$ s burst. The Raman amplifier has similar performance as FOPA for 30  $\mu$ s burst duration but lifts off with noticeable power penalty below 30  $\mu$ s burst. For bursts of 10  $\mu$ s and below sensitivity penalty between FOPA and Raman soars up to 3 dB. This relates to the fact that propagation delay in Raman amplified bursts suffers from severe transient effects for short burst durations. Sensitivity of different AUT's at BER =  $10^{-3}$  level shows standalone performance of different amplifiers. FOPA demonstrates improved performance in receiver sensitivity increasing it by >3 dB for short burst signal.

#### 4. Conclusion

We have experimentally demonstrated an employment of polarization insensitive FOPA with net gain up to 20 dB for amplification of bursts of 10 Gbps OOK signal in a 50 km reach PON architecture. We have compared the performance of a polarization insensitive FOPA with a commercial EDFA and a discrete Raman amplifier for amplification of non-burst signal as well as a range of signal burst durations from 70  $\mu$ s to 5  $\mu$ s. We found that in the non-burst scenario the FOPA and the Raman amplifier have introduced <1 dB penalty on the received signal power as compared to the EDFA. On the other hand, the Raman amplifier and the EDFA suffered from transient effects when amplifying signal bursts leading to BER degradation and eventually significant penalties on the receiver sensitivity. Thus, the EDFA and the discrete Raman amplifier introduced a receiver sensitivity penalty >3 dB when amplifying bursts shorter than 25  $\mu$ s and 15  $\mu$ s respectively. On the contrary, the FOPA has not distorted the signal burst waveforms and therefore the receiver sensitivity penalty in the FOPA case was <2 dB in all cases. Thus, an implementation of FOPA has allowed for a 7 dB better receiver sensitivity than EDFA in the worst case scenario of the 5  $\mu$ s burst duration. Overall, FOPA allows for a consistent performance for both continuous and burst traffic, while discrete Raman amplifiers and EDFAs can be prone to transient effects when amplifying signal bursts. Therefore, FOPA can allow for a larger power budget for extended reach PON than EDFAs and discrete Raman amplifiers with similar gain resulting in an improved reach and/or higher splitting ratio allowing for more customers to be served.

#### Funding

Engineering and Physical Sciences Research Council (FPA-ROCS (EP/R024057/1), UPON (EP/M005283/1)); H2020 Marie Skłodowska-Curie Actions (OPERNET and POLSAR (713694)).

#### Acknowledgement

The authors wish to thank Prof. Wlodek Forysiak and Dr. Md. Asif Iqbal for providing the Raman amplifier employed in this experimental work. To access the underlying data please see: <https://doi.org/10.17036/researchdata.aston.ac.uk.00000464>

#### Disclosures

The authors declare no conflicts of interests.

## References

1. T. Torounidis, P. A. Andrekson, and B. E. Olsson, "Fiber-optical parametric amplifier with 70-dB gain," *IEEE Photonics Technol. Lett.* **18**(10), 1194–1196 (2006).
2. A. Peric, S. Moro, N. Alic, A. J. Anderson, C. J. McKinstrie, and S. Radic, "Two-pump fiber-optic parametric amplifier with 66 dB gain and errorless performance," in *Frontiers in Optics* 2010 Oct 24 (p. FWW2). Optical Society of America
3. M. C. Ho, K. Uesaka, M. Marhic, Y. Akasaka, and L. G. Kazovsky, "200-nm-bandwidth fiber optical amplifier combining parametric and Raman gain," *J. Lightwave Technol.* **19**(7), 977–981 (2001).
4. J. M. C. Boggio, S. Moro, E. Myslivets, J. R. Windmiller, N. Alic, and S. Radic, "155-Nm Continuous-Wave Two-Pump Parametric Amplification," *IEEE Photonics Technol. Lett.* **21**(10), 612–614 (2009).
5. V. Gordienko, M. F. C. Stephens, A. E. El-Taher, and N. J. Doran, "Ultra-flat wideband single-pump Raman-enhanced parametric amplification," *Opt. Express* **25**(5), 4810–4818 (2017).
6. Z. Tong, C. Lundström, P. A. Andrekson, C. J. McKinstrie, M. Karlsson, D. J. Blessing, E. Tipsuwannakul, B. J. Puttnam, H. Toda, and L. Grüner-Nielsen, "Towards ultrasensitive optical links enabled by low-noise phase-sensitive amplifiers," *Nat. Photonics* **5**(7), 430–436 (2011).
7. S. Takasaka and R. Sugizaki, "Polarization insensitive fiber optical parametric amplifier using a SBS suppressed diversity loop," in *Optical Fiber Communication Conference (OFC 2016)*, paper M3D.4M. F.
8. M.F.C. Stephens, M. Tan, V. Gordienko, P. Harper, and N. J. Doran, "In-line and cascaded DWDM transmission using a 15 dB net-gain polarization-insensitive fiber optical parametric amplifier," *Opt. Express* **25**(20), 24312–24325 (2017).
9. V. Gordienko, F. Ferreira, A. Szabo, V. Ribeiro, C. Laperle, M. O. Sullivan, K. Roberts, A. Ellis, and N. Doran, "Characterisation of Novel Polarisation-Insensitive Configurations of Fibre Optical Parametric Amplifiers," in *European Conference on Optical Communications (ECOC 2019)*.
10. S. Bahae Mansoor and M. P. Hasselbeck, "Third-order optical nonlinearities," Chapter 5 Optical Kerr Effect., (Handbook of Optics, 2000).
11. A. Bogris and D. Syvridis, "Distributed optical parametric amplification at 1.3  $\mu\text{m}$ : Performance and applications in optical access networks," *IEEE Photonics Technol. Lett.* **24**(8), 694–696 (2012).
12. M. Ruffini, M. Achouche, A. Arbelaez, R. Bonk, A. Di Giglio, N. J. Doran, M. Furdek, R. Jensen, J. Montalvo, N. Parsons, T. Pfeiffer, L. Quesada, C. Raack, H. Rohde, M. Schiano, G. Talli, P. Townsend, R. Wessaly, L. Wosinska, X. Yin, and D. B. Payne, "Access and metro network convergence for flexible end-to-end network design [invited]," *J. Opt. Commun. Netw.* **9**(6), 524–535 (2017).
13. ITU-T, "G.9807.2 10 Gigabit-capable passive optical networks (XG(S)-PON): Reach extension," (2017).
14. ITU-T, "G.9807.1:10-Gigabit-capable symmetrical passive optical network (XGS-PON)," *ITU-T G-Series Recomm. E 41042*, 1–286 (2016).
15. S. Spolitis and G. Ivanovs, "Extending the reach of DWDM-PON access network using chromatic dispersion compensation," *IEEE Swedish Commun. Technol. Work. Swe-CTW* **2011**, 29–33 (2011).
16. K. Y. Cho, Y. Takushima, and Y. C. Chung, "Enhanced chromatic dispersion tolerance of 11Gbit/s RSOA-based WDM PON using 4-ary PAM signal," *Electron. Lett.* **46**(22), 1510–1512 (2010).
17. D. Lavery, S. Erkilinc, P. Bayvel, and R. I. Killey, "Recent progress and outlook for coherent PON," in *Optical Fiber Communication Conference (OFC 2018)* paper M3B.1
18. ITU-T Recommendation G.984.2 (2004), "Gigabit-capable passive optical networks (GPON): physical media dependent (PMD) layer specification".
19. D. Nessel, "PON Roadmap [Invited]," *J. Opt. Commun. Netw.* **9**(1), A71–A76 (2017).
20. M. Fujiwara and R. Koma, "Long-Reach and High-Splitting-Ratio WDM/TDM-PON Systems Using Burst-Mode Automatic Gain Controlled SOAs," *J. Lightwave Technol.* **34**(3), 901–909 (2016).
21. ITU-T G.984.6, (2012) "Gigabit-capable passive optical networks (G-PON): Reach extension Amendment 2", Recommendation.
22. N. Brandonisio, D. Carey, S. Porto, G. Talli, and P. D. Townsend, "Burst-mode FEC performance for PON upstream channels with EDFA optical transients," *22nd Conf. Opt. Netw. Des. Model. (ONDM 2018)* paper 190–193.
23. M. Dalla Santa, C. Antony, G. Talli, I. Krestnikov, and P. D. Townsend, "Burst-mode analysis of XGPON Raman reach extender employing quantum-dot lasers," *Electron. Lett.* **52**(13), 1157–1158 (2016).
24. B. J. Ainslie, "A Review of the Fabrication and Properties of Erbium-Doped Fibers for Optical Amplifiers," *J. Lightwave Technol.* **9**(2), 220–227 (1991).
25. C. R. Giles, J. R. Simpson, and E. Desurvire, "Transient gain and cross talk in erbium-doped fiber amplifiers," *Opt. Lett.* **14**(16), 880 (1989).
26. M. Shiraiwa, Y. Awaji, H. Furukawa, S. Shinada, B. J. Puttnam, and N. Wada, "Performance evaluation of a burst-mode EDFA in an optical packet and circuit integrated network," *Opt. Express* **21**(26), 32589 (2013).
27. B. Palsdottir, I. T. Monroy, L. K. Oxenløwe, and P. Jeppesen, "Impairments Due to Burst-Mode Transmission in a Raman-Based Long-Reach PON Link," *IEEE Photonics Technol. Lett.* **19**(19), 1490–1492 (2007).
28. L. Zhang, S. Wang, and C. Fan, "Transient analysis in discrete fiber Raman amplifiers," *Opt. Commun.* **197**(4–6), 459–465 (2001).
29. G. W. Lu, M. E. Marhic, and T. Miyazaki, "Burst-mode amplification of dynamic optical packets using fibre optical parametric amplifier in optical packet networks," *Electron. Lett.* **46**(11), 778–780 (2010).

30. S. Oda, H. Sunnerud, and P.A. Andrekson, "High efficiency and high output power fiber-optic parametric amplifier," *Opt. Lett.* **32**(13), 1776–1778 (2007).
31. V. Gordienko, M. F. C. Stephens, F. M. Ferreira, and N. J. Doran, "Raman-amplified pump and its use for parametric amplification and phase conjugation," *Opt. Fiber Technol.* **56**, 102183 (2020).
32. M. E. Marhic, K. K. Y. Wong, and L. G. Kazovsky, "Wide-band tuning of the gain spectra of one-pump fiber optical parametric amplifiers," *IEEE J. Sel. Top. Quantum Electron.* **10**(5), 1133–1141 (2004).
33. C. B. Gaur, F. Ferreira, V. Gordienko, V. Ribeiro, and N. J. Doran, "Demonstration of improved performance provided by FOPA for extended PON in burst-mode operation," in *European Conference on Optical Communications (ECOC 2019)*.
34. C. B. Gaur, F. Ferreira, V. Gordeinko, A. Iqbal, W. Forysiak, and N. Doran, "Comparison of Erbium, Raman and Parametric Optical Fiber Amplifiers for Burst Traffic in Extended PON," in *Optical Fiber Communication Conference (OFC 2020)* paper W4B.3.
35. H. Derbies, R. Brenot, J. Provost, G. Barbet, S. Poehlmann, W. Borkowski, R. Bonk, and T. Pfeiffer, "Quasi frequency drift suppression for burst mode operation in low-cost thermally-tuned TWDM-PON," in *Optical Fiber Communication Conference (OFC 2017)* paper .Th5A-5.
36. D. Mashimo, J. Sugawa, H. Ikeda, K. Minatozaki, and N. Matsudaira, "10-Gb/s Burst-mode receiver for fast settling time," in *Asia Communications and Photonics conference and Exhibition (ACP 2009)* paper. 1-2.
37. X. Yin, X. Z. Qiu, J. Gillis, J. Put, J. Verbrugghe, J. Bauwelinck, J. Vandewege, F. Blache, D. Lanteri, M. Achouche, H. Krimmel, D. Van Veen, and P. Vetter, "DC-coupled burst-mode receiver with high sensitivity, wide dynamic range and short settling time for symmetric 10G-GPONs," *Opt. Express* **19**(26), B594–B603 (2011).
38. G. P. Agrawal, "Nonlinear Fiber Optics," (Springer, Berlin, Heidelberg, 2004) Chap.4.
39. C.-J. Chen, J. Ye, W. S. Wong, and Y.-W. Lu, "Transient effects and their control in Raman optical amplifiers," *OWA1* (2014).
40. G. Bolognini and F. Di Pasquale, "Transient Effects in Gain-Clamped Discrete Raman Amplifier Cascades," *IEEE Photonics Technol. Lett.* **16**(1), 66–68 (2004).
41. S. Shakya, A. Supe, I. Lavrinovica, S. Spolitis, and J. Porins, "Different optical fiber nonlinear coefficient experimental measurements," *Int. Work. Fiber Opt. Access Network, FOAN 2016* 1–4 (2016).